# Cooperative Peak Shaving and Voltage Regulation in Unbalanced Distribution Feeders

Yifei Guo, Member, IEEE, Qianzhi Zhang, Student Member, IEEE, and Zhaoyu Wang, Member, IEEE

Abstract—This paper considers the co-operation of distributed generators (DGs), battery energy storage systems (BESSs) and voltage regulating devices for integrated peak shaving and voltage regulation in distribution grids through a co-optimization framework, which aims to minimize the operational costs while fulfilling the operational constraints of network and devices. To account for the uncertainties of load demand and generation, we then convert the co-optimization model into a two-stage stochastic program where state-of-charge (SoC) trajectories of BESSs and the operation of voltage regulating devices are optimized at the first stage for day-ahead scheduling (that determines the day-ahead bidding plans of utilities in the day-ahead market and the long-term voltage profile of feeders) while the reactive powers of DGs and BESSs are left at the second stage for potential intra-day scheduling to handle short-term voltage issues. The proposed co-optimization scheme is validated on the IEEE 37-node test feeder and compared with other practices.

*Index Terms*—Co-optimization, distributed generation (DG), battery energy storage system (BESS), peak shaving, two-stage stochastic programming, voltage/var regulation.

# I. INTRODUCTION

# A. Background and Motivation

■ N recent decades, a variety of government policy-based incentives have supported the growth in distributed generators (DG) such as wind, photovoltaic (PV), fuel cells, biomass, etc. Indeed, DGs bring technical, economic and environmental benefits; however, in turn, they may incur new operational stress, e.g., power quality and network congestion issues [1]. Battery energy storage system (BESS) is arguably the most promising solution to aid the integration of renewables since it can be deployed in a modular and distributed fashion [2]–[3]. Clearly, with a high penetration of DGs and BESSs, the real load profile may significantly deviate from the forecast, which will affect the utility companies' bidding behaviors in the wholesale electricity market and correspondingly, the feeder voltage profile will vary with the net load. Hence, in a nutshell, the ongoing deployment of DGs and BESSs poses challenges to energy management of distribution systems but facilitates its revolution to exploit renewables in a cost-effective way.

Peak shaving and voltage/reactive power (volt/var) regulation are two fundamental functionalities in distribution management systems where peak shaving is a process of flattening the load profile by shifting peak load demand to the off-peak

This work was supported by the U.S. Department of Energy Wind Energy Technologies Office under DE-EE-00087956. (*Corresponding author: Zhaoyu Wang.*)

The authors are with the Department of Electrical and Computer Engineering, Iowa State University, Ames, IA 50011 USA (e-mail:yifeig@iastate.edu; wzy@iastate.edu).

periods by leveraging energy storage and/or demand side management [6]; and the primary goal of volt/var regulation is, as the name suggests, maintaining the feeder voltages within a feasible range (e.g., 0.95–1.05 p.u. in ANSI Standard C84.1 [7]) by scheduling the voltage regulating devices, e.g., on-load tap changers (OLTCs), step-voltage regulators (SVRs) and capacitor banks (CBs) [8]. Moreover, the advanced four-quadrant inverter-interfaced DGs and BESSs are capable of providing fast and continuous volt/var support locally [4]–[5], which can significantly alleviate the work loads on the legacy devices.

Thanks to the conventional *separate* operation of peak shaving and volt/var regulation [8], a substantial body of studies have solely discussed either peak shaving or volt/var regulation for a long time; see [6] and [9]–[10] for surveys on these two isolate topics, respectively. However, the practical operation reveals the fact that they interact with each other due to the physical nature of power network: i) reshaping the load profile also reshapes the voltage profile, especially for some low-voltage (LV) feeders with high R/X ratios; and ii) regulating voltages can lower the peak load via reducing line losses and load demand (conservation voltage reduction) [11].

In light of this, the co-operation of peak shaving and voltage regulation becomes appealing since it can maximize the usage of DGs and storage, thereby unlocking additional benefits in terms of operational cost, power quality, supply reliability as well as network reinforcement, which, however, cannot be well accomplished by the traditional separate architectures.

# B. Literature Review

A few studies have addressed the co-operation between peak shaving and volt/var regulation, especially for the planning of DGs and BESSs considering the operation conditions. Several rule-based control algorithms have been proposed in [12]–[14]. However, they rely on the heuristic design without providing system-wide optimality guarantees.

Some studies have bridged the methodology gap by proposing optimization frameworks. In [15], the authors investigated the potential of BESSs in deferring upgrades needed to host a higher penetration of PV, where an optimal power flow (OPF) problem was formulated with the aim of mitigating voltage deviation and reducing peak load restricted by limited capital and operation and maintenance costs of BESSs. In [16], an optimization model that minimizes BESS cost, voltage deviation, voltage unbalance and peak demand charge together was built. It should be noted that the weight allocation on multiple heterogeneous objectives as in [15]–[16] is usually tricky. A short-term scheduling scheme of BESSs was proposed in [17]

to address peak shaving, volt/var regulation and reliability enhancement, simultaneously, resorting to solve an OPF program by Tabu search. In [18], a bi-level scheduling strategy was developed, consisting of the bidding in day-ahead market (DAM) to minimize overall the costs in supplying the net load and a real-time dispatch to compensate for the energy gap. However, [15]–[18] mainly focused on the operation of BESSs, neglecting the coordination with voltage regulating devices.

To address such issue, the efforts in [19]-[21] further have the legacy voltage regulating devices participate in the cooperation. In [19], a two-stage optimal dispatch framework for distribution grids with distributed wind was proposed, where the peak shaving and volt/var regulation are implemented in a successive coordinated fashion instead of the so-called cooptimization in a strict sense. In [20], a model predictive control scheme was proposed to minimize network losses or energy purchase cost whilst maintaining voltages within limits by co-optimizing the operation of OLTCs, PV inverters as well as BESSs in two timescales (1h and 15-min). The authors in [21] proposed an integrated framework for conservation voltage reduction and demand response to reduce the energy bills of customers. Besides, all of [19]-[21] addressed the prediction uncertainties of DGs and load by leveraging scenario-based stochastic programming techniques with one-stage [19], [21] or two-stage models [20]. However, the unbalanced case was not well addressed in [19]–[21]. <sup>1</sup>

## C. Contributions

In spirit, this work is close to [18]–[19] and [21] which consider a day-ahead multi-step scheduling of DGs and BESSs to enhance utilities' bidding strategies in the DAM. However, we contribute in the following distinct ways:

- 1) First, we for the first time propose a comprehensive cooptimization framework for an integrated peak shaving and volt/var regulation by scheduling DGs, BESSs and voltage regulating devices. This framework aims to minimize the overall operational costs including energy purchase, battery degradation, as well as wear and tear of tap changers and CBs, while satisfying the operational constraints. Especially, an unbalanced network with tap changers is considered where the multi-phase branch flow model is generalized and linearized in to incorporate phase-wise tap changers, rendering the problem computationally tractable.
- 2) Second, to account for the forecast uncertainties of renewables and load while relieving the conservative behavior of a robust decision, we propose to reformulate the problem into a two-stage stochastic program. It is noteworthy that, with this two-stage model, only the SoC trajectories of BESSs and voltage regulating devices will be actually implemented in day-ahead operation while reactive powers of DGs and BESSs are left for a re-scheduling.

<sup>1</sup>The unbalanced networks were considered in [15] and [16] but without the discrete voltage regulating devices. The works [20]–[21] used the second-order cone programming (SOCP) relaxation to convexify the OPF programs, which cannot be easily extended to unbalanced cases due to the mutual impedance of feeders. The semidefinite programming (SDP) relaxation used in [18] is applicable to unbalanced systems; however, it may be computationally expensive, especially in the presence of discrete variables.

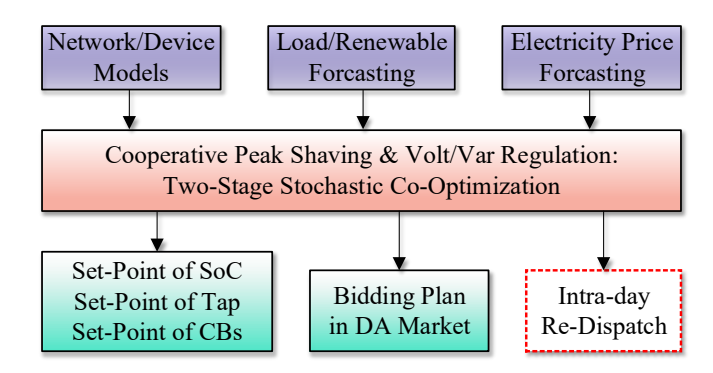


Fig. 1. Schematic diagram of the proposed day-ahead co-optimization framework for cooperative peak shaving and volt/var regulation. Though the intraday dispatch is not explicitly addressed in this work, the proposed two-stage stochastic programming methodology remains its potential in the second stage.

3) Last but not least, we demonstrate the proposed cooptimization unlocks additional revenue compared with the successive optimization method and also demonstrate that only relying on cost reduction does *not* necessarily lower the peak load. This implies an explicit peak load limit should be imposed in the co-optimization.

The rest of this paper is organized as follows. Section II presents the deterministic formulation of the co-optimization problem. In Section III, the optimization problem is reformulated as a two-stage stochastic program accounting for uncertainties. Section IV presents the numerical results with method comparison, followed by conclusions.

# II. PROBLEM FORMULATION

This section presents the problem formulation of the cooptimization framework for day-ahead cooperative peak shaving and volt/var regulation over the time horizon of 24 h with 1-h time resolution compatible with the DAM. Fig. 1 gives the overview of the proposed framework. Table I lists the major definitions of the symbols used throughout the paper<sup>2</sup>.

# A. Objective Function

The co-optimization framework aims to minimize the overall operational costs including energy purchase, batter degradation and wear-and-tear of tap changers and CBs during T, which is mathematically given as follows:

1) Electricity Purchase Cost:

$$C_{\text{ele}} := \sum_{t \in T} \lambda_{\text{ele},t} \Big( \text{Re} \left\{ \text{Tr}(S_{01,t}) \right\} + \sum_{(i,j) \in E} \text{Re} \left\{ \text{Tr}(z_{ij}l_{ij,t}) \right\} \Big) \Delta T \qquad (1)$$

where the first part is the feed-in power flow from the substation (that does not include the line losses) and the second term represents the total line losses.

 $^2\mathrm{Notations}:(\cdot)^*,\ (\cdot)^T$  and  $(\cdot)^H$  denote the element-wise conjugate, transpose and complex-conjugate transpose, respectively. For a vector,  $\mathrm{diag}(\cdot)$  denotes a diagonal matrix with the diagonal being  $(\cdot);$  for a matrix,  $\mathrm{diag}(\cdot)$  denotes the vector consisting of the diagonal entries of  $(\cdot).$  Re $\{\cdot\}$  and  $\mathrm{Im}\{\cdot\}$  denote the real part and imaginary part of a complex number;  $\mathbf{i}:=\sqrt{-1}.$   $\mathrm{Tr}(\cdot)$  denotes the matrix trace.

TABLE I NOTATIONS

Cymbolo	Description
Symbols $N := \{0\} \bigcup \{1,, n\}$	Description Set of buses
$N := \{0\} \cup \{1,, n\}$ $N^+$	
$F^{i} \subset N \times N$	Set of children buses of bus i
$\begin{bmatrix} E^i \subseteq N \times N \\ \Delta T \end{bmatrix}$	Set of branches Time resolution [h]
$T := \{1,, 24\}$	Set of time intervals
$\Phi_{ij} \subseteq \Phi_i \subseteq \{A, B, C\}$	Phase sets of bus $i$ and branch $(i, j)$
$\Xi^{ij} = \Xi^i = (\Xi, \Xi, \Xi)$	Set of scenarios
$V_n$	Nominal bus voltage
$\lambda_{ m ele}$	Predicted electricity price [\$/kWh]
$\lambda_{ m bat}$	Battery degradation cost [\$/kWh]
$\lambda_{\text{cell}}$	Battery cell price [\$/kWh]
$\lambda_{\text{tap}}$	Adjustment cost of tap changer [\$/time]
$V_{\text{cap}}$ $V_{\text{min}}$ $V_{\text{max}}$	Switching cost of CB [\$/time]
$I_{ij}^{\max}$ $\Delta Tap_{ij}$	Min./max. bus voltage magnitude limits Max. current limit of branch $(i, j)$
$\Delta Tap_{ij}$	Tap ratio change per step
$\Delta q_{i,\varphi}^c$	Capacity per bank of CB at bus $i, \varphi$
$\Delta K_{ij,\varphi}^{\max}$	Tap change limit per time step
$\Delta K_{ii}^{cot}$	Total tap change limit over $T$
$K_{ii}^{\min}, K_{ii}^{\max}$	Min./max. tap position at branch $(i, j)$
$B_{i,j}^{\text{mlax}}$	Number of CBs at bus $i, \varphi$
$K_{ij,\varphi}^{\min}, K_{ij,\varphi}^{\max}$ $B_{i,\varphi}^{\max}$ $\Delta B_{i,\varphi}^{\mathrm{tot}}$	Allowable changes of CB at bus $i, \varphi$
1 Peak	Peak load limit
$\overline{S}^{\mathrm{tr}}$	Transformer capacity
$egin{array}{c} rac{S}{S}_{i,arphi}^{g} \ rac{ar{arphi}}{ar{arphi}}^{g} \end{array}$	DG capacity at bus $i, \varphi$
$  \overline{p}_{i,arphi,t}^{g^{\prime\prime}}  $	Available power of renewable-based DG
$SoC^{\min}, SoC^{\max}$	Min/max operation limits of SoC
$\overline{S}_{i,\varphi}^{b}$	Battery power capacity at bus $i, \varphi$
$E_{i,\varphi}$	Battery energy capacity at bus $i, \varphi$
$\eta^{\text{ch}}, \eta^{\text{dc}}$	Battery charging/discharging efficiency
$s_i^b := [s_{i,\varphi}^b]_{\varphi \in \Phi_i}$	Complex BESS power injection at bus i
$s_i^c := [s_{i,\varphi}^{c,\varphi}]_{\varphi \in \Phi_i}$	Complex CB power injection at bus $i$
$s_i^g := [s_{i,\varphi}^g]_{\varphi \in \Phi_i}$	Complex DG power injection at bus $i$
$s_i^d := [s_i^l]_{\varphi \in \Phi_i}$	Complex load demand at bus i
$v_i \in \mathbb{H}^{ \Phi_i  \times  \Phi_i }$	Complex voltage at bus i
$z_{ij} \in \mathbb{C}^{ \Phi_{ij}  \times  \Phi_{ij} }$	Impedance matrix of branch $(i, j)$
$I_{ij} := [I_{ij,\varphi}]_{\varphi \in \Phi_{ij}}$	Complex line current from buses $i$ to $j$
$K_{ij} := [K_{ij,\varphi}]_{\varphi \in \Phi_{ij}}$	Tap position at branch $(i, j)$
$B_i := [B_i \cup B_i] \cup B_i$	Number of CBs connected to bus i
$S_{ij} \in \mathbb{C}^{ \Phi_{ij}  \times  \Phi_{ij} }$	Complex power flow from buses $i$ to $j$
$SoC_{i,\varphi}$	SoC of battery at bus $i, \varphi$

2) Battery Degradation Cost:

$$C_{\text{bat}} := \sum_{t \in T} \sum_{i \in N} \sum_{\varphi \in \Phi_i} \lambda_{\text{bat}} \left| \text{Re} \left\{ s_{i,\varphi,t}^b \right\} \right| \Delta T.$$
 (2)

3) Operational Cost of Tap Changer:

$$C_{\text{tap}} := \sum_{t \in T} \sum_{(i,j) \in E} \sum_{\varphi \in \Phi_{ij}} \lambda_{\text{tap}} \left| K_{ij,\varphi,t} - K_{ij,\varphi,t-1} \right|.$$
 (3)

4) Operational Cost of Capacitor Bank:

$$C_{\text{cap}} := \sum_{t \in T} \sum_{i \in N} \sum_{\varphi \in \Phi_i} \lambda_{\text{cap}} \left| B_{i,\varphi,t} - B_{i,\varphi,t-1} \right|. \tag{4}$$

Accordingly, the overall cost function is given by,

$$C := C_{\text{ele}} + C_{\text{bat}} + C_{\text{tap}} + C_{\text{cap}}.$$
 (5)

# B. Constraints

1) Multi-Phase Power Flow: The SOCP relaxation and SDP relaxation are usually used to convexify the nonlinear power flow equations. However, the SOCP relaxation cannot be readily applied to unbalanced cases due to the mutual impedance. Though the SDP relaxation can be used for

unbalanced networks, it does not scale well with the size of problem. Thus, it may be computationally expensive, especially in the presence of discrete variables. Moreover, the exactness of relaxation cannot be guaranteed. So, to make the optimization problem computationally tractable, we generalize the linear multi-phase branch flow model [23] to incorporate a tap changer, which is as, for any branch  $(i, j) \in E$ ,

$$\Lambda_{ij,t} = s_{j,t}^{l} - s_{j,t}^{g} - s_{j,t}^{b} - s_{j,t}^{c} + \sum_{k \in N_{j}^{+}} \Lambda_{jk,t}^{\Phi_{j}}, t \in T$$
(6)
$$S_{ij,t} = (aa^{H})^{\Phi_{ij}} \operatorname{diag}(\Lambda_{ij,t}), t \in T$$
(7)

$$S_{ij,t} = (aa^H)^{\Phi_{ij}} \operatorname{diag}(\Lambda_{ij,t}), t \in T$$
(7)

$$v_{i,t}^{\Phi_{ij}} = v_{j,t} - k_{ij,t}v_0^{\Phi_{ij}} + S_{ij,t}z_{ij}^H + z_{ij}S_{ij,t}^H, t \in T$$
 (8)

where  $a := [1, e^{-i2\pi/3}, e^{i2\pi/3}]^T$ ;  $k_{ij,t} := [k_{ij,t}]_{\varphi,\varphi' \in \Phi_{ij}}$ the entries as,

$$k_{ij,\varphi\varphi',t} = (K_{ij,\varphi,t} + K_{ij,\varphi',t})\Delta Tap_{ij}, \ \varphi, \varphi' \in \Phi_{ij}.$$
 (9)

It is understood that  $k_{ij,t} = diag(1,1,1)$  always holds for each branch without a tap changer.

Besides, to estimate the line losses, the line current can be approximately captured as, for any  $(i, j) \in E$ ,

$$\Lambda_{ij,t} = V_n \operatorname{diag}(a^{\Phi_{ij}} I_{ij,t}^H), \ t \in T$$
 (10)

$$l_{ij,t} = I_{ij,t}I_{ij,t}^H, \ t \in T.$$
 (11)

Keep in mind that the linear approximation in (6)–(11) establishes on the fact that the network is not too severely unbalanced and operates around the nominal voltage. This is widely believed to hold in practice if with effective voltage regulation.

2) Network Operation Security: The operational limits of bus voltage and line current are as follows:

$$(V^{\min})^2 \le \operatorname{diag}(v_{i,t}) \le (V^{\max})^2, \ i \in N, t \in T$$
 (12)

$$diag(l_{ij,t}) \le (I_{ij}^{max})^2, \ (i,j) \in E, t \in T.$$
 (13)

3) Peak Load Demand: Additionally, we consider a hard constraint of net peak load during a day,

$$\operatorname{Re}\left\{\operatorname{Tr}(S_{01,t})\right\} + \sum_{(i,j)\in E} \operatorname{Re}\left\{\operatorname{Tr}(z_{ij}l_{ij,t})\right\} \le Peak, \ t \in T.$$
(14)

Imposing this explicit constraint is of great significance for effective peak shaving because only relying on cost reduction does not necessarily lower the peak load, which will be demonstrated later.

4) Substation Transformer: The transformer capacity limit is expressed as,

$$\| [\operatorname{Re} \{ \operatorname{Tr}(S_{01,t}) \} \|_{2} \le \overline{S}^{tr}, t \in T$$
 (15)

where to reduce the computation complexity, line losses are neglected here since this constraint generally is not truly binding considering the feed from DGs and the slight overloading of transformer is allowed for a short period.

5) Tap Changer: The operational constraints of tap changer over branch are given by, for any  $(i, j) \in E$  and  $\varphi \in \Phi_{ij}$ ,

$$K_{ij,\varphi}^{\min} \le K_{ij,\varphi,t} \le K_{ij,\varphi}^{\max}, \ K_{ij,\varphi,t} \in \mathbb{Z}, t \in T$$
 (16)

$$|K_{ij,\varphi,t} - K_{ij,\varphi,t-1}| \le \Delta K_{ij,\varphi}^{\max}, \ t \in T$$
(17)

$$\sum_{t \in T} |K_{ij,\varphi,t} - K_{ij,\varphi,t-1}| \le \Delta K_{ij,\varphi}^{\text{tot}}$$
(18)

where (16) denotes the tap position limits; (17) constrains the tap change during a sampling time interval; and (18) constrains the total operation times of tap changers during T.

6) Capacitor Bank: The operational constraints of capacitor banks are given as, for any bus  $i \in N$  and  $\varphi \in \Phi_i$ ,

$$\operatorname{Re}\{s_{i,\varphi,t}^c\} = 0, t \in T \tag{19}$$

$$\operatorname{Im}\{s_{i,\varphi,t}^c\} = B_{i,\varphi,t} \Delta q_{i,\varphi}^c, \ t \in T$$
 (20)

$$0 \le B_{i,\varphi,t} \le B_{i,\varphi}^{\max}, \ B_{i,\varphi,t} \in \mathbb{Z}, \ t \in T$$
 (21)

$$\sum_{t \in T} |B_{i,\varphi,t} - B_{i,\varphi,t-1}| \le \Delta B_{i,\varphi}^{\text{tot}}$$
(22)

where (19) denotes the total reactive power injected by CBs; (20) constrains the maximum number of CBs; (21) constrains the maximum switching times of CB units during T.

7) Battery Energy Storage: In this paper, we consider the lithium-ion battery—one of the most popular options today. If we limit the battery operation within certain depth of discharge region to avoid the overcharge and over-discharge, there is a constant marginal cost for the cycle depth increase. In this way, the battery degradation cost can be prorated with respect to charged and discharged energy into a per-kWh cost [24],

$$\lambda_{\text{bat}} = \frac{\lambda_{\text{cell}}}{2M(SoC^{\text{max}} - SoC^{\text{min}})}$$
 (23)

where M is the number of cycles that the battery could be operated within  $[SoC^{\min}, SoC^{\max}]$ .

The model and operational constraints of a BESS at  $\varphi \in \Phi_i$ of bus  $i \in N$  can be expressed as,

$$\operatorname{Re}\{s_{i,\omega,t}^{b}\} = b_{i,\omega,t}^{\operatorname{dc}} - b_{i,\omega,t}^{\operatorname{ch}}, \ t \in T$$
(24)

$$\operatorname{Re}\{s_{i,\varphi,t}^{b}\} = b_{i,\varphi,t}^{\operatorname{dc}} - b_{i,\varphi,t}^{\operatorname{ch}}, \ t \in T$$

$$0 \le b_{i,\varphi,t}^{\operatorname{ch}} \le \mu_{i,\varphi,t} \cdot \overline{S}_{i,\varphi}^{b}, \ t \in T$$
(24)

$$0 \le b_{i,\varphi,t}^{\text{dc}} \le (1 - \mu_{i,\varphi,t}) \cdot \overline{S}_{i,\varphi}^{b}, \ t \in T$$

$$\mu_{i,\varphi,t} \in \{0,1\}, \ t \in T$$

$$(26)$$

$$\mu_{i,\varphi,t} \in \{0,1\}, \ t \in T \tag{27}$$

$$SoC_{i,\varphi,t} = SoC_{i,\varphi,t-1} + \left(b_{i,\varphi,t}^{\mathrm{ch}} \eta^{\mathrm{ch}} - \frac{b_{i,\varphi,t}^{\mathrm{dc}}}{\eta^{\mathrm{dc}}}\right) \frac{\Delta T}{\overline{E}_{i,\varphi}}, \ t \in T$$

$$SoC^{\min} \le SoC_{i,\varphi,t} \le SoC^{\max}, \ t \in T$$
 (29)

$$SoC_{i,\varphi,0} = SoC_{i,\varphi,24}$$

$$(30)$$

$$\left\| \left[ \operatorname{Re}\{s_{i,\varphi,t}^{b}\} \right] \right\|_{2} \leq \overline{S}_{i,\varphi}^{b}, \ t \in T$$
 (31)

where  $\mu_{i,\varphi,t}$  denotes the indicator variable representing the charge or discharge status, respectively. Constraints (24)–(27) represent the real power model of a BESS. Constraint (28) represents the physical model of SoC of a BESS while (29)-(30) represent its operational constraints. As shown in (30), the SoC at the beginning and the end of a day will be equal so that the framework can periodically operate. (31) constrains the apparent power of BESS converter that restricts the real and reactive power in a coupling way.

8) Inverter-Based DG: A four-quadrant inverter-interfaced DG at  $\varphi \in \Phi_i$  of bus  $i \in N$  is modeled by

$$\operatorname{Re}\left\{s_{i,\varphi,t}^{g}\right\} = \overline{p}_{i,\varphi,t}^{g}, t \in T \qquad (32)$$

$$\left\| \left[ \operatorname{Re} \{ s_{i,\varphi,t}^g \} \right] \right\|_2 \le \overline{S}_{i,\varphi}^g, \ t \in T$$
 (33)

where it is assumed the PV system operates with the maximum power tracking mode (track the available power  $\overline{p}_{i,o,t}^g$ ).

Clearly, for each bus i that does not have CB, BESS or DG installation, we have  $s_{i,t}^c = 0$ ,  $s_{i,t}^g = 0$  or  $s_{i,t}^b = 0$ , respectively.

# C. Linearization and Compact Formulation

The objectives (2)–(4) and constraints (18) and (22) contain the sum of absolute terms with respect to the tap position and CBs, which are not tractable for off-the-shelf solvers. Thus, we linearize them by introducing the auxiliary variables  $K^+_{ij,\varphi}, K^-_{ij,\varphi}\,B^+_{i,\varphi}$  and  $B^-_{i,\varphi}$ . Then, constraint (18) can be equivalently rewritten as,

$$K_{ij,\varphi,t} - K_{ij,\varphi,t-1} = K_{ij,\varphi,t}^+ - K_{ij,\varphi,t}^-$$
 (34)

$$\sum_{t \in T} \left( K_{ij,\varphi,t}^+ + K_{ij,\varphi,t}^- \right) \le \Delta K_{ij,\varphi}^{\text{tot}} \tag{35}$$

$$K_{ij,\varphi,t}^{+} \ge 0, K_{ij,\varphi,t}^{-} \ge 0, K_{ij,\varphi,t}^{+}, K_{ij,\varphi,t}^{-} \in \mathbb{Z}.$$
 (36)

Similarly, constraint (21) becomes,

$$B_{i,\varphi,t} - B_{i,\varphi,t-1} = B_{i,\varphi,t}^+ - B_{i,\varphi,t}^-$$
 (37)

$$\sum_{t \in T} \left( B_{i,\varphi,t}^+ + B_{i,\varphi,t}^- \right) \le \Delta B_{i,\varphi}^{\text{tot}} \tag{38}$$

$$B_{i,\varphi,t}^+ \ge 0, B_{i,\varphi,t}^- \ge 0, B_{i,\varphi,t}^+, B_{i,\varphi,t}^- \in \mathbb{Z}.$$
 (39)

For BESSs, similar linearization has been done in (24)–(27). Correspondingly, the cost functions  $C_{\text{tap}}$ ,  $C_{\text{cap}}$  as well as  $C_{\text{bat}}$ can be rewritten as,

$$C_{\text{tap}} = \sum_{t \in T} \sum_{(i,j) \in E} \sum_{\varphi \in \Phi_{i,j}} \lambda_{\text{tap}} \left( K_{ij,\varphi,t}^+ + K_{ij,\varphi,t}^- \right)$$
(40)

$$C_{\text{cap}} = \sum_{t \in T} \sum_{i \in N} \sum_{\varphi \in \Phi_i} \lambda_{\text{cap}} \left( B_{i,\varphi,t}^+ + B_{i,\varphi,t}^- \right)$$
(41)

$$C_{\text{bat}} = \sum_{t \in T} \sum_{i \in N} \sum_{\varphi \in \Phi_i} \lambda_{\text{bat}} \left( b_{i,\varphi,t}^{\text{ch}} + b_{i,\varphi,t}^{\text{dc}} \right) \Delta T.$$
 (42)

Finally, the optimization problem is abstractly expressed as,

(DP): 
$$\min_{u \in \mathcal{U}} C(u)$$
 (43a)

subject to 
$$g(u) \le 0$$
: 
$$\begin{cases} (12)-(17),(21) \\ (25)-(27),(29),(31) \\ (33),(35),(36),(38),(39) \end{cases}$$
 
$$h(u) = 0$$
: 
$$\begin{cases} (1),(5),(6)-(11),(19) \\ (20),(24),(30),(32) \\ (34),(37),(40)-(42) \end{cases}$$
 (43c)

$$h(u) = 0: \begin{cases} (1),(5),(6)-(11),(19) \\ (20),(24),(30),(32) \\ (34),(37),(40)-(42) \end{cases}$$
(43c)

where u is the compact decision vector of all the decisions;  $\mathcal{U}$ is the Cartesian product of real, complex and integer number sets, which characterizes u in an element-wise manner.

So far, the deterministic problem formulation (DP) has been given in (43), which is inherently a mixed-integer second-order cone program (MISOCP) that can be efficiently handled by the off-the-shelf solvers, e.g., CPLEX, MOSEK, etc.

<sup>&</sup>lt;sup>3</sup>To allow for real power curtailment, oen can replace "=" by "≤" in (33).

# III. STOCHASTIC PROGRAMMING FORMULATION

The day-ahead operation scheduling establishes on the load, renewable generation and electricity price, etc. However, due to various uncertainties, e.g. stochastic nature of the load and renewables, it is difficult to forecast them with very high accuracy. Therefore, we consider the forecast uncertainties of load and renewables by converting the deterministic optimization program DP into a two-stage stochastic program, while allowing for intra-day re-dispatching of reactive power resources.

#### A. Scenario Generation and Reduction

The load consumption prediction error is calculated based on a truncated normal distribution [29]. The solar power generation is dependent on the incident solar irradiance, while the irradiance significantly depends on the cloud coverage condition. Therefore, the solar irradiance prediction error is modeled by introducing a correction factor to the prediction  $\overline{Ir}$  with a clear weather, following a normal distribution that depends on the given cloud coverage level [30],

$$Ir = \overline{Ir}(1 - \varepsilon), \ \varepsilon = \left[\text{Norm}(\mu_{\varepsilon}, \sigma_{\varepsilon})\right]_0^1$$
 (44)

where  $[\cdot]_0^1$  denotes the projection operation onto the set [0, 1]. Based on the known probability distributions, Monte-Carlo simulation is conducted to create a required number of scenarios for solar irradiance and load and then they are reduced to a given number of scenarios by the backward reduction method, of which more details can be referred to [31]–[32].

## B. Two-Stage Stochastic Programming Formulation

First, we split  $u\in\mathcal{U}$  into two groups, i.e.,  $u:=\{x,y\}$  and  $\mathcal{U}:=\mathcal{X}\times\mathcal{Y}$  where

- x represents the decision variables associated with the charging/discharging of BESSs, operation of tap changers and operation of CBs (without the power flow); and
- y consisting of all the remaining ones.

Correspondingly, the cost function and constraints in OPF-d can be reconstructed as,

$$C(u) \Rightarrow C_1(x) + C_2(y) \tag{45}$$

$$h(u) \Rightarrow h_1(x) = 0 \cap h_2(x, y) = 0$$
 (46)

$$q(u) \Rightarrow q_1(x) < 0 \cap q_2(x, y) < 0$$
 (47)

$$u \in \mathcal{U} \Rightarrow x \in \mathcal{X} \cap y \in \mathcal{Y}$$
 (48)

where  $C_1(x)$  corresponds to  $C_{\text{bat}} + C_{\text{tap}} + C_{\text{cap}}$  while  $C_2(y)$  corresponds to  $C_{\text{ele}}$ .

Then, define a realization of stochastic scenario as  $\xi:=\left\{p_{i,\varphi,t}^g,s_{i,\varphi,t}^d\right\}_{i\in N,t\in T}$ , a two-stage stochastic counterpart of DP can be formulated as,

(SP): 
$$\min_{x \in \mathcal{X}} C_1(x) + \mathbb{E}_{\xi} \left\{ \min_{y \in \mathcal{Y}} C_2(y; \xi) \right\}$$
 (49a)

subject to 
$$h_1(x) = 0$$
 (49b)

$$g_1(x) \le 0 \tag{49c}$$

$$h_2(x, y; \xi) = 0 \tag{49d}$$

$$q_2(x, y; \xi) = 0$$
 (49e)

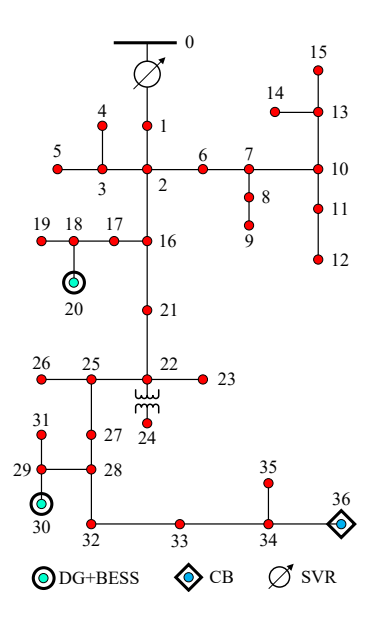


Fig. 2. Single-line diagram of IEEE 37-node test feeder. The original feeder is modified to include two phase-wise PV panels at Buses 20 and 30 with the rated capacities of 200 kVA and 300 kVA per phase. Two phase-wise BESSs with 500 kW/1500kWh and 300 kVA/900kWh power/energy ratings per phase at Buses 20 and 30, respectively. Besides, a CB with a rated capacity of 50 kVAr/unit and 100 kVAr in total per phase is installed at Bus 36.

where x corresponds to the first-stage (here-and-now) decisions before the realization of  $\xi$  and y corresponds to the second-stage (wait-and-see) corrective actions under a given realization of  $\xi$ . To be more clear, the independent control variables at the first stage include charging/discharging power of BESSs  $\operatorname{Re}\{s_{i,\varphi,t}^b\}$ , operation trajectories of tap changers  $K_{ij,t}$  and operation trajectories of CBs  $s_{i,t}^c$ ; and the second-stage control variables are the reactive powers of BESSs and DGs, i.e.,  $\operatorname{Im}\{s_{i,\varphi,t}^b\}$  and  $\operatorname{Im}\{s_{i,\varphi,t}^g\}$ .

# C. Deterministic Equivalent

Representing the uncertainties through a finite scenario set  $\Xi := \{\xi_1,...,\xi_{|\Xi|}\}$  with the probability distribution  $\rho_1,...,\rho_{|\Xi|}$ , the approximate deterministic equivalent problem of SP in the extensive form can be given as,

(SP-d): 
$$\underset{x \in \mathcal{X}, y_k \in \mathcal{Y}}{\text{minimize}} C_1(x) + \sum_{k=1}^{|\Xi|} \rho_k C_2(y_k; \xi_k)$$
 (50a)

subject to 
$$h_1(x) = 0$$
 (50b)

$$g_1(x) \le 0 \tag{50c}$$

$$h_2(x, y_k; \xi_k) = 0, k = 1, ..., |\Xi|$$
 (50d)

$$g_2(x, y_k; \xi_k) = 0, k = 1, ..., |\Xi|$$
 (50e)

which is inherently an extensive MISOCP program that can be also directly handled by conic programming solvers.

# IV. NUMERICAL RESULTS

The proposed co-optimization methodologies are tested on a modified IEEE 37-node test feeder (see Fig. 2) [25]. The SVR has an operation range of [0.9,1.1] p.u. with  $\pm 16$  tap positions (i.e.,  $K^{\min} = -16$ ,  $K^{\max} = 16$  and  $\Delta Tap = 0.2/32$ ). The

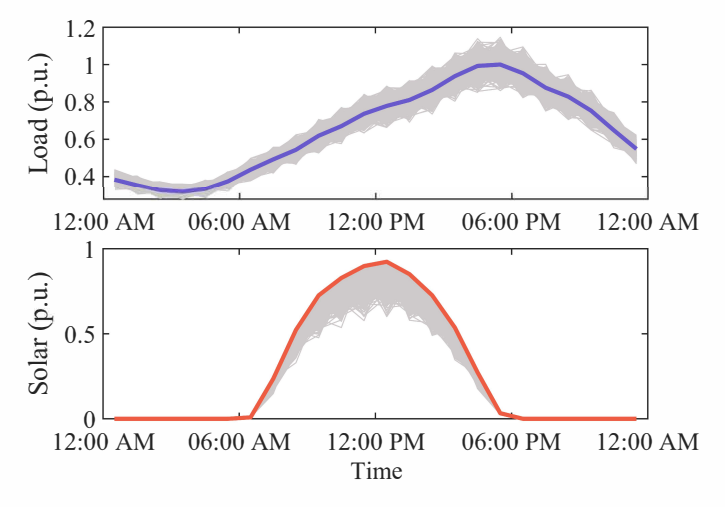


Fig. 3. Load and solar generation profiles (1-h resolution). The thick lines represent the predicted profiles while others are generated stochastic scenarios.

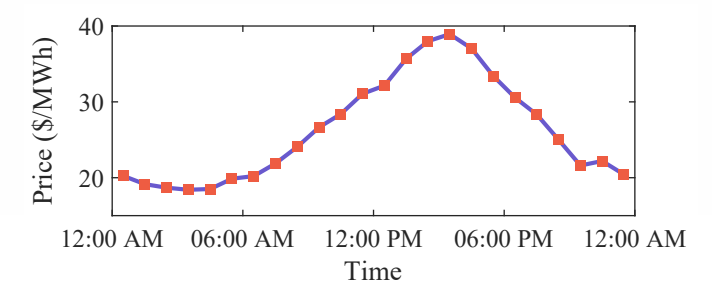


Fig. 4. Day-ahead locational marginal price in central Iowa at July 3rd 2017 obtained from historical MISO market dataset.

Lithium Manganese Oxide battery is considered for the simulation with a cell price of 0.5/Wh and M = 10,000 cycles when the average cycle depth of discharge is 60% [24]. Accordingly,  $SoC^{\min} = 0.2$  and  $SoC^{\max} = 0.8$ . The per-unit costs associated with operation of the tap changer and CB are set as 1.40\\$/time and 0.24\\$/time which can be adjusted as per the switching risk assessment of utilities [26]. The daily load profile of a real distribution feeder in Iowa, U.S. and a solar generation time series generated by a testbed [27] are used as the predictions of load and maximum available solar generation (see Fig. 3). The locational marginal price obtained from historical MISO market dataset [28] is used as the forecasted electricity price in DAM (Fig. 4). For uncertainty modeling, as discussed before, it is assumed the random load prediction error follows the truncated normal distribution where the mean value is the forecasted load, the standard deviation is 5% and the truncation bound is set as  $\pm 15\%$ , respectively; the solar irradiance correction factor follows the normal distribution with mean value  $\mu_{\varepsilon} = 10\%$  and standard deviation  $\sigma_{\varepsilon} = 5\%$ . These parameters can be tuned per the given real data.

# A. Co-Optimization v.s. Successive Optimization

In this section, we perform a comparison between the proposed co-optimization (cooperative peak shaving and volt/var regulation) and the successive coordinated optimization proposed in [19] to demonstrate the unlocked additional benefits by the proposed co-operation. For the successive optimization,

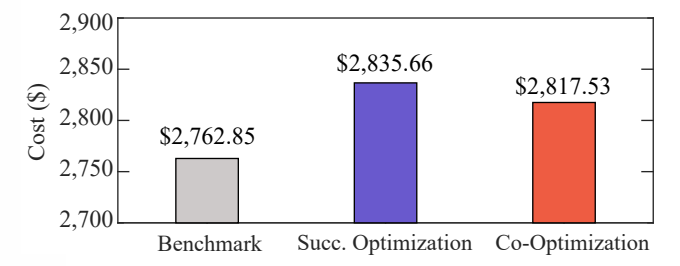


Fig. 5. Operational cost comparison with different operation strategies.

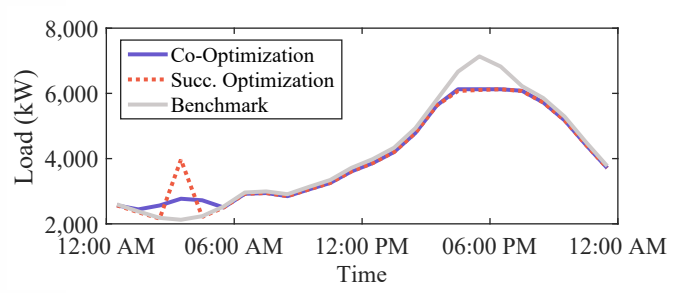


Fig. 6. Peak load performance with different operation strategies. To conduct a fair comparison (same peak load), the successive optimization strategy with a peak limit (without line losses) of 5,700 MW is first tested and then the resultant actual peak load after voltage regulation (6,100 MW, including line losses) is set as the peak limit in the co-optimization.

the peak shaving and the volt/var optimization are performed in a successive way; for the benchmark, the distribution system operates without peak shaving and volt/var regulation. For the sake of clarity, this comparison is performed on a deterministic case. To better illustrate the effectiveness of the proposed method, the benchmark load demand in [25] is scaled up by four. As shown in Fig. 5, the operational costs with different optimization strategies are compared. It shows that the cooptimization strategy reduces the operational cost compared with the successive optimization one with the same peak load and voltage limits. Seen from Fig. 6, to achieve peak shaving, the load during peak times will be shifted to 12:00 AM-06:00 AM with relatively low prices by scheduling the BESSs. Utilities will thus purchase more electricity for this period. Besides, as shown in Figs. 7 (b) and (c), the voltage profiles with the two optimization methods are effectively regulated within the limits [0.95,1.05] p.u. but by comparison, the co-optimization results in smoother voltage variations. The benchmark has the lower operational costs because it does not include any operational costs of BESSs and voltage regulating devices but most bus voltages significantly violate the lower limit while the peak load stays high.

# B. Merit of an Explicit Peak Load Constraint

In this subsection, we examine the necessity of a hard and explicit peak load limit constraint in the co-optimization. As shown in Fig. 8, only relying on the cost reduction (Case B) does not effectively lower the peak load because the imposed operational cost of BESSs is more expensive than cost savings by leveraging the ToU price, though it does reduce the overall operational costs of the system. Without considering BESS costs in the optimization, it is observed that the peak load can

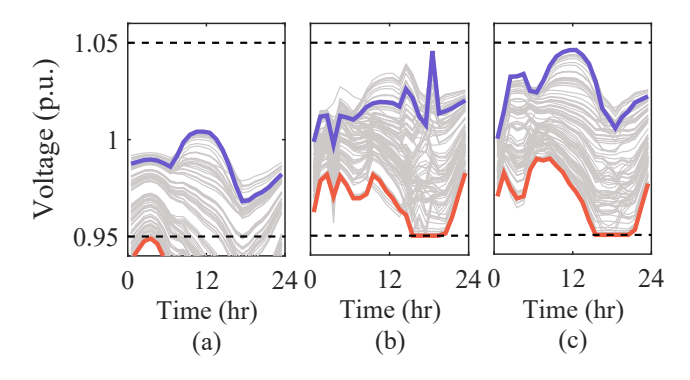


Fig. 7. Voltage performance with different operation strategies. (a) Benchmark; (b) successive optimization; (c) co-optimization. Each line represents a phase-wise voltage magnitude of a bus. The thick lines highlight the lowest and highest bus voltages within a day.

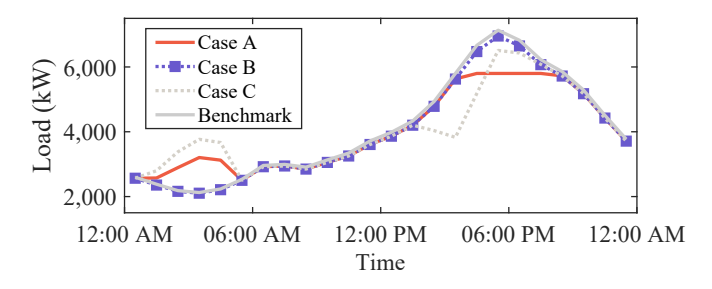


Fig. 8. Peak load performance with different operation strategies where in Case A, the co-optimization strategy is carried out with a peak load limit of 5,800 MW; in Case B, the peak load limit is relaxed; and in Case C, the peak load limit and the operational costs of BESSs are both relaxed.

be slight reduced. But, consider, if we have sufficient available load shifting capability, there will be a trend that all the load will be shifted/aggregated to the periods with the lowest price. Therefore, there will be a new (and higher) peak at 04:00 AM. This demonstrates the merit of an explicit constraint on peak load in the optimization problem.

# C. Deterministic Optimization v.s. Stochastic Optimization

Here, the comparison between the deterministic optimization and (singe-stage and two-stage) stochastic optimization methods is carried out to demonstrate the value of stochastic programming. 1,000 random scenarios of load and solar power time-series are generated as shown in Fig. 3 and are then reduced to 15 representative scenarios, which strives for a balance between performance and computational complexity. Fig. 9 compares the voltage performance among different optimization methods. 100 new scenarios are generated to test the performance of different methods under uncertainties and we record the highest and lowest value voltage magnitude of all buses after 100 random Monte-Carlo simulations. It can be observed that some voltage buses (especially for Phase C) with the deterministic optimization (DP) violate the lower limit under some scenarios since it does not consider the uncertainties in the optimization. The single-stage stochastic optimization strategy schedules all the controllable devices in one stage together considering the uncertain prediction errors and therefore, it alleviates the voltage violations in Phase C but there

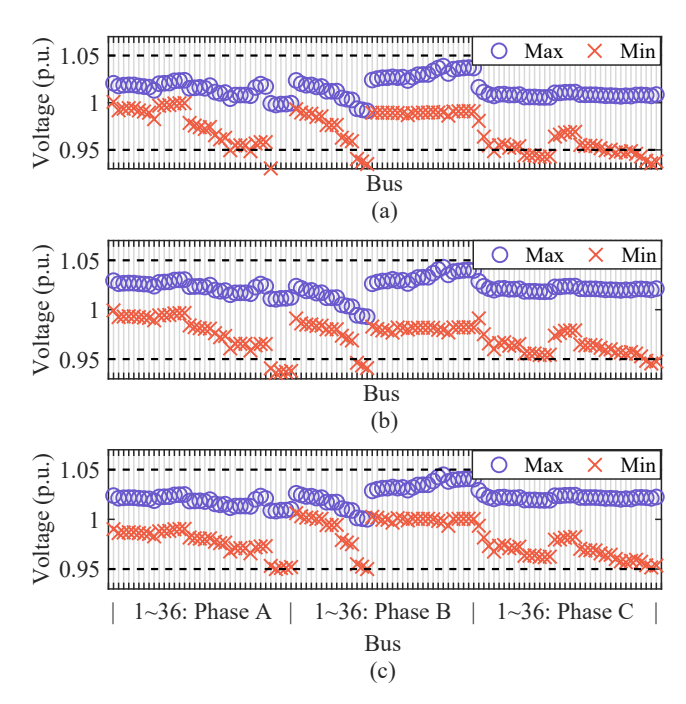


Fig. 9. Voltage performance (min./max. magnitude) with (a) deterministic optimization, (b) singe-stage stochastic optimization and (c) two-stage stochastic optimization where the maximum and minimum values of all (phase-wise) bus voltages during a day among the 100 test scenarios are presented.

are still several bus voltages lower than 0.95 p.u. In comparison, the two-stage stochastic optimization framework regulates all the bus voltages within the ANSI limit since it considers the uncertainties and allows a re-scheduling of reactive powers of BESSs and solar inverters, thereby exhibiting better robustness. This justifies the necessity of the intra-day re-scheduling of available controllable devices.

Fig. 10 gives the comparison in terms of peak shaving performance. It can be observed that, with the deterministic optimization, the peak load violates 6,000 kW in most of scenarios with the highest peak of 6,856.4 kW; the single-stage stochastic optimization alleviates the violation with the highest peak of 6,450.1 kW. By contrast, the two-stage optimization can effectively regulate the peak load (maximum peak load 6,087.5 kW) because it effectively reduces the network losses under a given case by re-dispatching the reactive power of BESSs and solar inverters. This again validates the merit of stochastic optimization and the necessity of re-dispatch.

# V. CONCLUSION

This paper addresses the day-ahead cooperative operation of peak shaving and voltage regulation in an unbalanced distribution through a joint optimization framework. We then consider the uncertainties of load and solar by converting the co-optimization model into a two-stage stochastic program. The numerical results show that the proposed co-optimization framework brings more cost benefits than the successive optimization method while effectively regulating the voltages and peak load within the limits. Further, due to the consideration of uncertainties and the enabled re-dispatch, the proposed two-stage stochastic programming method facilitates robust operations. Besides, we also verify the necessity of an explicit peak

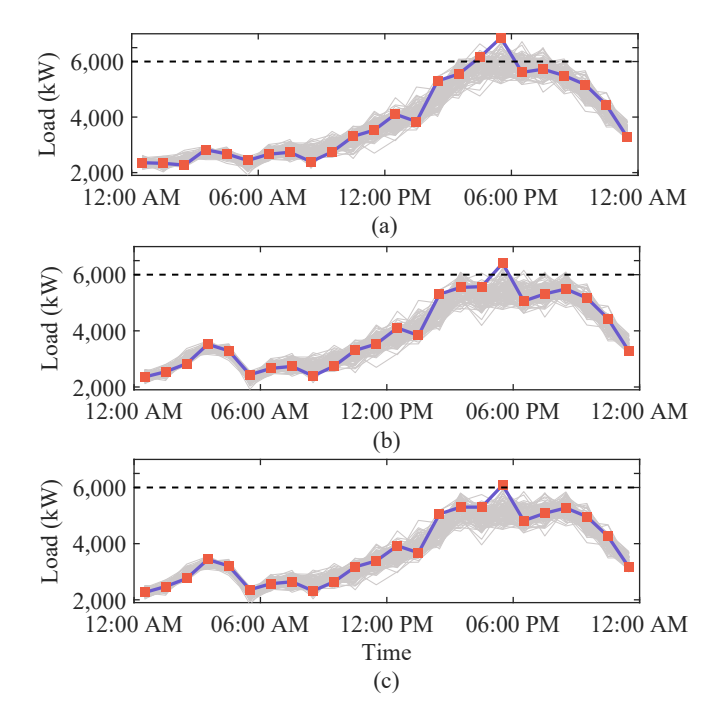


Fig. 10. Peak load performance with deterministic, one-stage stochastic and two-stage stochastic optimization. (a) deterministic; (b) one-stage stochastic optimization; (c) two-stage stochastic optimization. Each line represents the real power load of distribution system under a given stochastic scenario. The thick line represents the scenario with the highest peak load.

load constraint in the optimization for effective peak shaving. The future work will focus on the intra-day real-time dispatch to better track the system variations.

## REFERENCES

- S. Kakran and S. Chanana, "Smart operations of smart grids integrated with distributed generation: A review," *Renew. Sustain. Energy Rev.*, vol. 81, pp. 524–535, Jan. 2018.
- [2] B. Dunn, H. Kamath, and J.-M. Tarascon, "Electrical energy storage for the grid: A battery of choices," *Science*, vol. 334, no. 6058, pp. 928-935, 2011.
- [3] S. Comello, S. Reichelstein, "The emergence of cost effective battery storage. *Nature Commun.*, vol. 10 no.1, pp. 1–9, 2019.
- [4] Y. Guo, Q. Wu, H. Gao, X. Chen, J. Østergaard, and H. Xin, "MPC-based coordinated voltage regulation for distribution networks with distributed generation and energy storage system," *IEEE Trans. Sustain. Energy*, vol. 10. no. 4, pp. 1731–1739, Oct. 2019.
- [5] A. Colmenar-Santos, C. Reino-Rio, D. Borge-Diez, and E. Collado Fernandez, "Distributed generation: A review of factors that can contribute most to achieve a scenario of DG units embedded in the new distribution networks," *Renew. Sustain. Energy Rev.*, vol. 59, pp. 1130–1148, 2016.
- [6] M. Uddin, M. F. Romlie, M. F. Abdullah, S. A. Halim, A. H. A. Bakar, and T. C. Kwang, "A review on peak load shaving strategies," *Renew. Sustain. Energy Rev.*, vol. 82, pp. 3323-3332, Feb. 2018.
- [7] American National Standard for Electric Power Systems and Equipment -Voltage Ratings (60 Hz), ANSI C84.1–2011 Std.
- [8] R. Singh, R. Uluski, J. T. Reilly, et al, "Foundational Report Series: Advanced Distribution Management Systems for Grid Modernization, DMS Industry Survey," Argonne Nat. Lab., Lemont, IL, USA, Tech. Rep., Apr. 2017.
- [9] H. Sun, Q. Guo, et al., "Review of challenges and research opportunities for voltage control in smart grids," *IEEE Trans. Power Syst.*, vol. 34, no. 4, Jul. 2019.
- [10] K. E. Antoniadou-Plytaria, I. N. Kouveliotis-Lysikatos, P. S. Georgilakis, and N. D. Hatziargyriou, "Distributed and decentralized voltage control of smart distribution networks: Models, methods, and future research," *IEEE Trans. Smart Grid*, vol. 8, no. 6, pp. 2999–3008, Nov. 2017.

[11] J. Carden and D. Popovic, "Closed-loop Volt/Var optimization: Addressing peak load reduction," *IEEE Power Energy Mag.*, vol. 16, no. 2, pp. 67–75. Mar. 2018

- [12] J. Zupačič, E. Lakić, T. Medved, and A. Gubina, "Advanced peak shaving control strategies for battery storage operation in low voltage distribution network," in *Proc. IEEE Manchester PowerTech*, Jun. 2017.
- [13] M. J. E. Alam, K. M. Muttaqi, and D. Sutanto, "Mitigation of rooftop solar PV impacts and evening peak support by managing available capacity of distributed energy storage systems," *IEEE Trans. Power Syst.*, vol. 28, no. 4, pp. 3874–3884, Nov. 2013.
- [14] Y. Yang, H. Li, A. Aichhorn, J. Zheng, and M. Greenleaf, "Sizing strategy of distributed battery storage system with high penetration of photovoltaic for voltage regulation and peak load shaving," *IEEE Trans. Smart Grid*, vol. 5, no. 2, pp. 982–991, Mar. 2014.
- [15] J. Tant, F. Geth, D. Six, P. Tant, and J. Driesen, "Multiobjective battery storage to improve PV integration in residential distribution grids," *IEEE Trans. Sustain. Energy*, vol. 4, no. 1, pp. 182–191, Jan. 2013.
- [16] N. Jayasekara, M. A. S. Masoum, and P. J. Wolfs, "Optimal operation of distributed energy storage systems to improve distribution network load and generation hosting capability," *IEEE Trans. Sustain. Energy*, vol. 7, no. 1, pp. 250–261, Jul. 2016.
- [17] M. Sedghi, A. Ahmadian, and M. Aliakbar-Golkar, "Optimal storage planning in active distribution network considering uncertainty of wind power distributed generation," *IEEE Trans. Power Syst.*, vol. 31, no. 1, pp. 304–316, Jan. 2016.
- [18] Y. Zheng, et al., "Optimal operation of battery energy storage system considering distribution system uncertainty," *IEEE Trans. Sustain. En*ergy, vol. 9, no. 3, pp. 1051–1060, Jul. 2018.
- [19] B. Zhou, D. Xu, K. W. Chan, C. Li, Y. Cao, and S. Bu, "A two-stage framework for multiobjective energy management in distribution networks with a high penetration of wind energy," *Energy*, vol. 135, pp. 754–766, Jul. 2017.
- [20] R. Zafar, J. Ravishankar, J. E. Fletcher, and H. R. Pota, "Multi-timescale model predictive control of battery energy storage system using conic relaxation in smart distribution grids," *IEEE Trans. Power Syst.*, vol. 33, no. 6, pp. 7152–7161, Nov. 2018.
- [21] M. S. Hossan and B. Chowdhury, "Integrated CVR and demand response framework for advanced distribution management systems," *IEEE Trans. Sustain. Energy*, vol. 11, no. 1, pp. 534–544, Jan. 2020.
- [22] Z. Taylor, et al., "Customer-side SCADA-assisted large battery operation optimization for distribution feeder peak load shaving," *IEEE Trans.* Smart Grid, vol. 10, no. 1, pp. 992-1004, Jan. 2019.
- [23] L. Gan and S. H. Low, "Convex relaxations and linear approximation for optimal power flow in multiphase radial networks," in *Proc. Power* Syst. Comput. Conf., 2014, pp. 1–9.
- [24] Y. Shi, B. Xu, D. Wang, and B. Zhang, "Using battery storage for peak shaving and frequency regulation: Joint optimization for superlinear gains," *IEEE Trans. Power Syst.*, vol. 33. no. 3, pp. 2882-2894, May 2018.
- [25] IEEE, "37 node distribution test feeder." Aug. 2017. [Online]. Available: https://ewh.ieee.org/soc/pes/dsacom/testfeeders/
- [26] P. Li, H. Ji, C. Wang, J. Zhao, G. Song, F. Ding, and J. Wu, "A coordinated control method of voltage and reactive power for active distribution networks based on soft open point," *IEEE Trans. Sustain. Energy*, vol. 8, no. 4, pp. 1430–1442, Oct. 2017.
- [27] C. Holcomb, Pecan Street Inc.: A test-bed for NILM, in International Workshop on Non-Intrusive Load Monitoring, 2012. [Online]. Available: https://www.pecanstreet.org/
- [28] "MISO Market Data: Historical LMP," Accessed: Sep., 2017. [Online]. Available: https://www.misoenergy.org/markets-and-operations/real-time—market-data/market-reports/#nt=
- [29] N. Lu, R. Diao, R. P. Hafen, N. Samaan and Y. Makarov, "A comparison of forecast error generators for modeling wind and load uncertainty," in *Proc. IEEE PES Gen. Meeting*, Vancouver, BC Canada, pp. 1-5, 2013.
- [30] R. Torquato, Q. Shi, W. Xu, et al., "A Monte Carlo simulation platform for studying low voltage residential networks," *IEEE Trans. Smart Grid*, vol. 5, no. 6, pp. 2766–2776, Jul. 2014.
- [31] J. Dupačová, N. Gröwe-Kuska, and W. Römisch, "Scenario reduction in stochastic programming: An approach using probability metrics," *Math. Programm.*, vol. A 95, pp. 493–511, 2003.
- [32] Z. Wang, J. Wang, B. Chen, M. Begovic, and Y. He, "MPC-based voltage/var optimization for distribution circuits with distributed generators and exponential load models," *IEEE Trans. Smart Grid*, vol. 5, no. 5, pp. 2412–2420, Sep. 2014.